Arterivirus replicase processing : regulatory cascade or Gordian knot?

Aken, A.T. van

Chapter 7

Proteolytic maturation of replicase polyprotein pp1a by the nsp4 main protease is essential for equine arteritis virus replication and includes internal cleavage of nsp7

Danny van Aken, Jessika Zevenhoven-Dobbe, Alexander E. Gorbalenya and Eric J. Snijder, (2006)

Journal of General Virology **87** (Pt 12): 3473-3482

Chapter 7

Abstract

The positive-sense RNA genome of the arterivirus equine arteritis virus (order *Nidovirales*) encodes the partially overlapping replicase polyproteins pp1a (1,727 amino acids) and pp1ab (3,175 amino acids). Previously, three viral proteases were reported to cleave these large polyproteins into 12 non-structural proteins (nsps). The chymotrypsin-like viral main protease residing in nsp4 is responsible for eight of these cleavages. Processing of the C-terminal half of pp1a (the nsp3-8 region) was postulated to occur following either of two alternative proteolytic pathways (the "major" and the "minor" pathway; Wassenaar *et al.* (1997) J. Virol. 71, 9313-9322). Here, the importance of these two pathways was investigated by using a reverse genetics system and inactivating each of the cleavage sites by site-directed mutagenesis. For all these pp1a cleavage sites, mutations that prevented cleavage by the nsp4 protease were found to block or severely inhibit EAV RNA synthesis. Furthermore, our studies identified a novel nsp4 cleavage site (Glu-1575/Ala-1576) that is located within nsp7 and is conserved in arteriviruses. The N-terminal nsp7 fragment (nsp7α) derived from this cleavage was detected in lysates of both EAV-infected cells and cells transiently expressing pp1a. Mutagenesis of the novel cleavage site in the context of an EAV full-length cDNA clone proved to be lethal, underlining that the highly regulated, nsp4-mediated processing of the C-terminal half of pp1a is a crucial event in the arterivirus life cycle.

Introduction

Equine arteritis virus (EAV), the prototype of the arterivirus family of enveloped, positive-sense RNA viruses (Snijder & Meulenberg, 2001; Siddell *et al.*, 2005), has a polycistronic genome of about 12.7 kb. Together with the *Coronaviridae* and *Roniviridae*, the *Arteriviridae* are classified in the order *Nidovirales* (Snijder *et al.*, 2005; Spaan *et al.*, 2005; Gorbalenya *et al.*, 2006). Nidoviruses share a similar genome organization, use common transcriptional and (post)-translational strategies to regulate their gene expression and have a conserved array of homologous replicase domains.

The EAV replicase proteins (nsp1-12) are encoded by two large, 5'-proximal open reading frames, ORF1a and ORF1b, that are translated from the genome RNA, with expression of ORF1b involving a ribosomal frameshift just upstream of the ORF1a termination codon (den Boon *et al.*, 1991). The genome translation products are the polyproteins pp1a (1,727 amino acids) and pp1ab (3,175 amino acids) that are processed by three internal virus-encoded proteases. Nsp1 and nsp2 each contain an autoprotease domain that rapidly liberates these products from both polyproteins, whereas the nsp4 or "main protease" (Snijder *et al.*, 1996; Ziebuhr *et al.*, 2000; Barrette-Ng *et al.*, 2002) is responsible for the processing of all cleavage sites in the remaining part of pp1a and pp1ab, nsp3-8 and nsp3-12, respectively (Fig. 7.1) (Wassenaar *et al.*, 1997; Snijder & Meulenberg, 1998; Ziebuhr *et al.*, 2000).

Previously, based on experiments with infected cells and pp1a expression systems, processing of nsp3-8 (and possibly also the nsp3-8 moiety of nsp3-12) was proposed to follow either of two alternative proteolytic pathways (Fig. 7.1; (Wassenaar *et al.*, 1997; Snijder & Meulenberg, 1998; Ziebuhr *et al.*, 2000)). In the majority of precursors, the nsp4/5 junction was found to be cleaved, producing the nsp3-4 and nsp5-8 processing intermediates ("major pathway"; (Wassenaar *et al.*, 1997)). Subsequently, the latter product

was cleaved at the nsp7/8 site only, whereas the nsp5/6 and nsp6/7 sites were found to remain unprocessed. In the alternative, “minor pathway", cleavage of the nsp4/5 site was not observed, but instead the nsp5/6 and nsp6/7 junctions in the nsp3-8 and nsp4-8 intermediates were processed. Wassenaar *et al.* (Wassenaar *et al.*, 1997) demonstrated that cleavage of the nsp4/5 site depends on the presence of cleaved nsp2 as a cofactor, but the exact mechanism of this potential regulatory switch in EAV replicase processing remains to be elucidated.

The crystal structure of the nsp4 protease (Barrette-Ng *et al.*, 2002) confirmed that its catalytic triad His-1103, Asp-1129 and Ser-1184 indeed is grafted onto a two ß-barrel chymotrypsin-like fold (Snijder *et al.*, 1996). The enzyme contains a C-terminal extension (about 45 amino acids in EAV nsp4), which is found in all nidoviral chymotrypsin-like proteases despite their very limited overall sequence similarity (Anand *et al.*, 2002; Yang *et al.*, 2003; Ziebuhr *et al.*, 2003; Smits *et al.*, 2006). Recent studies on this domain of EAV nsp4 revealed that it is not required for proteolytic activity *per se*, but may be important at another level than catalysis (van Aken *et al.*, 2006b).

The arterivirus main protease displays a preference for Glu at the P1 position and a small amino acid (Gly, Ser or Ala) at the P1’ position (using the nomenclature of Schechter and Berger (Schechter & Berger, 1967)) of the substrate (Snijder *et al.*, 1996; Ziebuhr *et al.*, 2000), a specificity typical of picornavirus 3C proteases and related 3C-like enzymes of other RNA viruses (Gorbalenya & Snijder, 1996; Ryan & Flint, 1997). As for other positive-sense RNA viruses (Ding & Schlesinger, 1989; Bartenschlager *et al.*, 1994; Rose *et al.*, 1995; Hardy *et al.*, 2002), the proteolytic maturation of the replicase is assumed to be crucial for the assembly and function of the enzyme complex that drives arterivirus RNA synthesis. However, replicase processing in arteriviruses and other nidoviruses has mainly been studied in expression systems and the amount of data from infected cells is very limited. The fact that protease inhibitors can block coronavirus replication supported the general importance of pp1a/pp1ab processing for viral RNA synthesis (Kim *et al.*, 1995) (Yang *et al.*, 2005), but the importance of individual cleavages has not been addressed in any detail. Reverse genetics studies recently demonstrated that certain cleavages in the relatively poorly conserved N-terminal domain of the coronavirus replicase pp1a/pp1ab polyproteins may be dispensable for replication (Denison *et al.*, 2004). In contrast, inactivation of two of the three nsp4 cleavage sites (nsp9/10 and nsp11/12) in the most conserved, ORF1b-encoded part of the EAV replicase polyprotein completely inactivated viral RNA synthesis, whereas mutagenesis of the third cleavage site (nsp10/11) allowed RNA synthesis but blocked the production of infectious progeny (van Dinten *et al.*, 1999).

The importance of the nsp4-specific cleavages in the ORF1a-encoded part of the EAV replicase polyprotein has not been investigated. Mutations blocking each of these cleavage sites were previously documented (Snijder *et al.*, 1996; Wassenaar *et al.*, 1997), but at that time the reverse genetics system required to test their effect and the importance of the two pp1a processing pathways in the context of the viral life cycle was not yet available. We now report that all nsp4-mediated cleavages in EAV pp1a are critical for viral RNA synthesis. In addition, our studies identified a novel cleavage site for the nsp4 protease, which is located within the nsp7 subunit and appears to be conserved among arteriviruses. The products resulting from this cleavage had previously gone unnoticed due to technical reasons. Mutagenesis of the novel cleavage site in the context of the EAV full-length cDNA clone proved to be lethal to the virus.

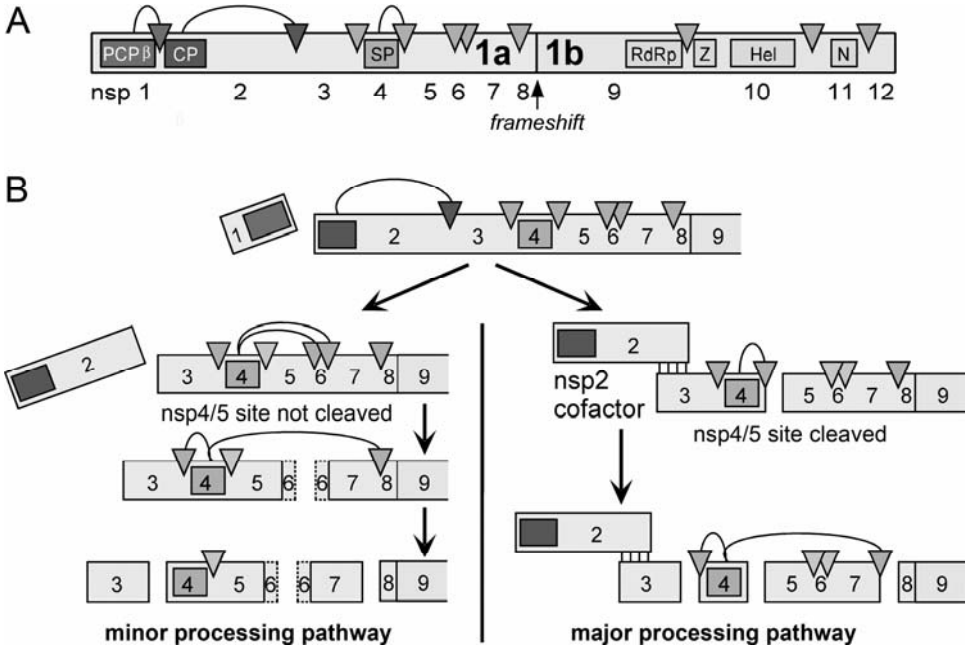

Figure 7.1. Proteolytic processing of the EAV replicase. (**A**) Processing map of the 3,175-amino acid EAV replicase polyprotein pp1ab. The three EAV proteases (PCPβ, CP and SP), their cleavage sites and the EAV nsp nomenclature are depicted. PCPβ nsp1 papain-like cysteine protease; CP, nsp2 cysteine protease; SP, nsp4 serine protease; RdRp, RNA-dependent RNA polymerase; Z, zinc finger; Hel, helicase; N, nidovirus-specific endoribonuclease (NendoU). (**B**) Overview of the two alternative processing pathways proposed for EAV pp1a (Wassenaar *et al.*, 1997). The association of cleaved nsp2 with nsp3-8 (and probably also nsp3-12) was postulated to be a cofactor in the cleavage of the nsp4/5 site by the nsp4 protease (major pathway) (Wassenaar *et al.*, 1997). Alternatively, in the absence of nsp2, the nsp4/5 junction was found to remain uncleaved but the nsp5/6 and nsp6/7 sites were processed (minor pathway). Adapted from (Barrette-Ng *et al.*, 2002).

Materials and methods

Virus, cells and antisera

The EAV Bucyrus strain (Doll *et al.*, 1957) was grown in baby hamster kidney cells (BHK-21) as described previously (de Vries *et al.*, 1992). Vaccinia virus recombinant vTF7-3 (Fuerst *et al.*, 1986), which produces the T7 RNA polymerase, was propagated in rabbit kidney (RK-13) cells. The anti-nsp4 and anti-nsp7-8 rabbit sera were originally named anti-4M and anti-5, respectively (Snijder *et al.*, 1994).

cDNA constructs

Mutations were engineered using standard PCR techniques (Landt *et al.*, 1990). Amplified regions were fully sequenced and standard recombinant DNA techniques were used (Sambrook *et al.*, 1989) to introduce mutations into plasmid pL1a and EAV full-length cDNA clone pEAV1a (see below). Previously described mutations were Ser-1184→Ile,

replacing the active site Ser of the nsp4 protease, and five mutations replacing the P1 residue of each of the nsp4 cleavage sites in pp1a (nsp3/4 to nsp7/8; Fig. 7.1 and Table 1): Glu-1064, Glu-1268, Glu-1430, Glu-1452, and Glu-1677 (Snijder *et al.*, 1996; Wassenaar *et al.*, 1997). Newly generated mutations are listed in Table 1. Most of these were accompanied by a few additional silent mutations to engineer restriction sites that could be used as marker. The wild-type (wt) pL1a expression construct (Snijder *et al.*, 1996) contains the full-length EAV ORF1a (encoding pp1a, which equals nsp1-8) downstream of a T7 promoter and encephalomyocarditis virus internal ribosomal entry site. Mutated PCR fragments were introduced in pL1a using the unique restriction sites *Spe*I (nt 3763 in the genome) and *Eco*RV (nt 4265), and mutations were verified by sequence analysis. pEAV1a is a derivative of EAV full-length cDNA clone pEAV030 (van Dinten *et al.*, 1997; van Aken *et al.*, 2006b).

Transient expression and protein analysis

EAV pp1a was transiently expressed from expression plasmid pL1a in RK-13 cells using the recombinant vaccinia virus/T7 RNA polymerase expression system (Fuerst *et al.*, 1986) and liposome-mediated transfection (Lipofectamine Plus; Invitrogen) as described previously (van Aken *et al.*, 2006b). Proteins synthesised in transfected cells were labelled with 200 µCi/ml [^{35}S]-Promix (Amersham) from 5 to 10 h post vaccinia virus infection. Protocols for cell lysis and immunoprecipitation have been described previously (Snijder *et al.*, 1994). Proteins were separated by SDS-PAGE according to Laemmli (Laemmli, 1970) and the amount of [^{35}S]-label incorporated into protein bands was measured using a phosphorimager (Biorad Molecular Imager FX) and quantified using Biorad Quantity One software.

EAV reverse genetics

The methods used for transcription of EAV full-length cDNA clones and for transfection of infectious RNA into BHK-21 cells by electroporation have been described previously (van Dinten *et al.*, 1997). RNA quality -and yield were assessed by agarose gel electrophoresis. Virus replication in transfected cells and transfection efficiency were assayed by indirect immunofluoresence assays (IFA) (van der Meer *et al.*, 1998) using a rabbit antiserum directed against replicase subunit nsp3 and a mouse monoclonal antibody recognizing the nucleocapsid (N) protein. Plaque assays were carried out according to previously described protocols (Snijder *et al.*, 2003).

Bioinformatics

Multiple sequence alignments of a representative set of nsp7 sequences from diverse arteriviruses were generated using the MUSCLE program (Edgar, 2004), taking into consideration the phylogenetic clustering of the *Arteriviridae* (Snijder *et al.*, 2005; Spaan *et al.*, 2005). The analysis was done using the Viralis platform that integrates software tools and a relational database of virus genome sequences (A. E. Gorbalenya *et al.*, in preparation).

Tabel 1. EAV mutants used in this study and their phenotype.

Virus	Wild-type sequence[a]	Mutated sequence[b]	Amino acid substitution	IFA nsp3	IFA N	Titer at 13 h p.t.
EAV-1a wt	n.a.	n.a.	n.a.	+	+	$1x10^8$
E1064P	GAA GGG CTA	**CCC** GGG CTA	Glu-1064 → Pro	-	-	$<2x10^1$
E1268P	AGA GAG AGC	AG**G CCT** AGC	Glu-1268 → Pro	-	-	$<2x10^1$
E1430P	GAG GGA GGA	**CCC** GG**G** GGA	Glu-1430 → Pro	-	-	$<2x10^1$
E1452P	GAG AGT CTC	**CCA** AGC **TTG**	Glu-1452 → Pro	-	-	$<2x10^1$
E1677P	GAA GGC CTA	**CCC** GG**G** CTA	Glu-1677 → Pro	-	-	$<2x10^1$
E1677Q	GAA GGC CTA	**CAG** GGC CT**G**	Glu-1677 → Gln	-	-	$<2x10^1$
G1678A	GAA GGC CTA	GAA **GCG** CT**T**	Gly-1678 → Ala	+	+	$9x10^6$
G1678N	GAA GGC CTA	GAA **AAC** CT**T**	Gly-1678 → Asn	+	+	$5x10^6$
E1575A	GAA GAA GCC	GAA **GCA** GCC	Glu-1575 → Ala	-[c]	-[c]	$<2x10^1$
E1574A/ E1575A	GAA GAA GCC	**GCA** **GCA** GCC	Glu-1574 → Ala Glu-1575 → Ala	-	-	$<2x10^1$

[a] Mutated codons are underlined.
[b] Mutated codons are underlined; nucleotide changes are indicated in boldface.
[c] Reversion observed at 24 h p.t. in one experiment.

Results and discussion

Both the major and minor pp1a processing pathways are critical for EAV replication

Previously, EAV replicase pp1a processing was studied using the recombinant vaccinia virus/T7 RNA polymerase expression system, which was found to faithfully reproduce the cleavages that occur in infected cells. In this expression system, replacement of the fully conserved P1 Glu residue with Pro was shown to completely abolish processing of each of the five nsp4 cleavage sites in the nsp3-8 region of pp1a (Snijder *et al.*, 1996; Wassenaar *et al.*, 1997). Of these cleavages the one at the nsp4/5 site was previously designated a marker for the major processing pathway, whereas processing of the nsp5/6 and nsp6/7 sites was assumed to be unique to the minor pathway (Fig. 7.1). To assess the significance of individual cleavages in the context of the EAV life cycle, and the importance of the major and minor processing pathways in general, we introduced each of these five P1 mutations into an EAV full-length cDNA clone (Table 1). Anticipating a lethal effect of these P1 replacements (van Dinten *et al.*, 1999), the nsp7/8 site was chosen to engineer and test some additional, less drastic mutations. P1 residue Glu-1677 was replaced with Gln, which is found at this position at the EAV nsp10/11 junction. The P1' residue Gly-1678 was replaced with Ala, which is found at this position in various cleavage sites in other arteriviruses (Ziebuhr *et al.*, 2000), and Asn, a mutation that will be discussed in more detail below.

BHK-21 cells were transfected with full-length EAV RNA transcripts specifying these mutations and the phenotype of the mutant viruses was analyzed at the end of the first replication cycle (13-15 h post transfection). Later time points were also monitored to screen for the possible occurrence of reversion in the case of nonviable or crippled mutants. The initial screening was done on the basis of a double IFA using antisera recognizing replicase subunit nsp3 and the nucleocapsid (N) protein, which are reliable indicators for

the synthesis of genome and subgenomic mRNA7, respectively (Snijder *et al.*, 2003). In addition, transfected cell culture supernatants were harvested and used for plaque assays to determine infectious progeny titers.

On the basis of these assays, it was concluded that each of the five P1 Glu→Pro mutations abolished all detectable viral RNA synthesis (Table 1). In repeated experiments, for none of these mutants reversion was observed (monitored up to 48 h post transfection). Although we cannot formally exclude additional detrimental effects of these P1 replacements that might affect virus replication, these results and our previous studies (Wassenaar *et al.*, 1997) would strongly suggest that both the major and minor processing pathways (Fig. 7.1) are critical for EAV RNA synthesis.

Of the additional nsp7/8 cleavage site mutants, both P1' mutants (G1678A and G1678N) were viable and produced infectious progeny, although titers were somewhat lower than for the wt control (Table 1). The wt-like phenotype of the G1678N mutant was rather unexpected, since thus far Asn has not been found at the P1' position of any (predicted) arterivirus nsp4 cleavage site (Ziebuhr *et al.*, 2000). The nonviable phenotype of mutant E1677Q (Table 1) indicated that Gln is not tolerated at the P1 position of the nsp7/8 site, despite its presence of this residue at this position of another EAV cleavage site, the nsp10/11 junction (van Dinten *et al.*, 1999).

Analysis of nsp7/8 mutants in a transient expression system

To assess their effect on proteolysis of the nsp7/8 junction in some detail, the novel mutations were transferred to pp1a expression vector pL1a. Mutant proteins were transiently expressed, metabolically labelled and processing was analyzed by immunoprecipitation with an anti-nsp7-8 serum. This serum specifically brings down the nsp5-8 and nsp5-7 products, of which the latter is thought to be a processing end product (Fig. 7.1; (Wassenaar *et al.*, 1997)). Thus, the nsp7/8 cleavage efficiency could be assessed by comparing the amount of immunoprecipitated nsp5-8 and nsp5-7 (Fig. 7.2A). As negative controls, the previously described nsp7/8 site P1 mutant (E1677P; (Wassenaar *et al.*, 1997)) and a nsp4 protease active site mutant (S1184I; (Snijder *et al.*, 1996)) were included.

The analysis confirmed that, as expected, the P1' Gly→Ala mutation in viable mutant G1678A did not significantly affect proteolysis of the nsp7/8 junction (Fig. 7.2A, lane 7). However, for the second viable P1' mutant (G1678N), the Gly→Asn mutation reduced the nsp7/8 cleavage with approximately 80%. Strikingly, the level of inhibition was comparable to that in nonviable mutant E1677Q (compare Fig. 7.2A, lanes 5 and 6; the Glu-1677→Gln mutation caused a nsp5-8-specific mobility shift). This suggests that in the latter mutant the Glu-1677→Gln replacement in nsp7 may have had additional detrimental effects, which e.g. could have affected the functionality of nsp7 or one of its precursors.

Surprisingly, an analysis of the low molecular weight region of the gel shown in Fig. 7.2 revealed additional differences between these mutants. In the lanes of the wt control and all nsp7/8 cleavage site mutants, the anti-nsp7-8 serum brought down an approximately 14-kDa protein (indicated as p14 in Fig. 7.2) that was conspicuously absent in the lane of nsp4 active site mutant S1184I (Fig. 7.2A, lane 2), suggesting that its presence depended on the activity of the nsp4 protease. The generation of this product appeared unaffected by nsp7/8 cleavage site mutations. Moreover, mutant E1677P (Fig. 7.2, lane 4), in which the nsp7/8 cleavage is completely blocked, displayed a second band

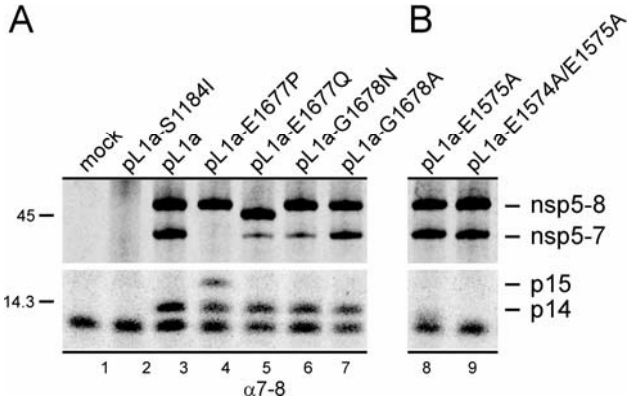

Figure 7.2. Expression and processing of the full-length EAV pp1a using the recombinant vaccinia virus/T7 RNA polymerase expression system (see Materials and methods). Immunoprecipitation analysis of pL1a and the pL1a nsp7/8 cleavage site mutants (**A**) and the pL1a nsp7α/7β (**B**) after a 5 h interval labelling using a nsp7-8 antiserum. Because nsp2 is present in this system, pp1a processing occurs mainly via the major pathway, although small amounts of pp1a are processed via the minor pathway. Mock-transfected cells, wt pL1a, and the pL1a-S1184I nsp4 protease mutant (**A**) were included as controls. The position of the molecular mass markers used during SDS-PAGE and the various processing products are indicated.

of approximately 15 kDa (p15). Both products were brought down by an anti-nsp7-8 antiserum (Fig. 7.2), but only the ~15-kDa product from mutant E1677P was recognized by an anti-nsp8 serum (data not shown), suggesting that it is a C-terminal pp1a fragment consisting of nsp8 (~5.5 kDa) and a C-terminal fragment of nsp7. This raised the possibility that nsp7 (~25 kDa) was cleaved internally and that p14 in Fig. 7.2 is in fact the corresponding N-terminal part of the protein. *In vitro* cleavage assays using EAV nsp4 and substrates from the nsp6-8 region were recently described to yield processing products of similar size (van Aken *et al.*, 2006a).

Evidence for the generation of smaller products from the nsp7 region in EAV-infected cells

To investigate whether the novel small products were also produced in EAV-infected cells, the low-molecular weight region of long exposures of previous immunoprecipitation analyses were scrutinized (Snijder *et al.*, 1994). Indeed, when using the anti-nsp7-8 serum (Fig. 7.3A, right panel), but not when using the anti-nsp8 serum (Fig. 7.3A, left panel), at least one and possibly two minor products in the 13-16 kDa size range were detected (indicated by arrows). Previously, these products may have gone unnoticed due to their small size, low abundance and the large amount of the 14-kDa N protein, which is brought down due to its interaction with protein A molecules on the *Staphylococcus aureus* cells used for immunoprecipitation (de Vries *et al.*, 1992). Note that the relatively late appearance of these small products correlated with the accumulation of nsp5-7 and nsp7, suggesting that they may originate from processing of either of these larger intermediates. Also in Western blot experiments (Fig. 7.3B), the same small products were recognized by the anti-nsp7-8 serum but not by the anti-nsp8 serum, again suggesting the generation of previously unrecognized products from the EAV nsp7 region.

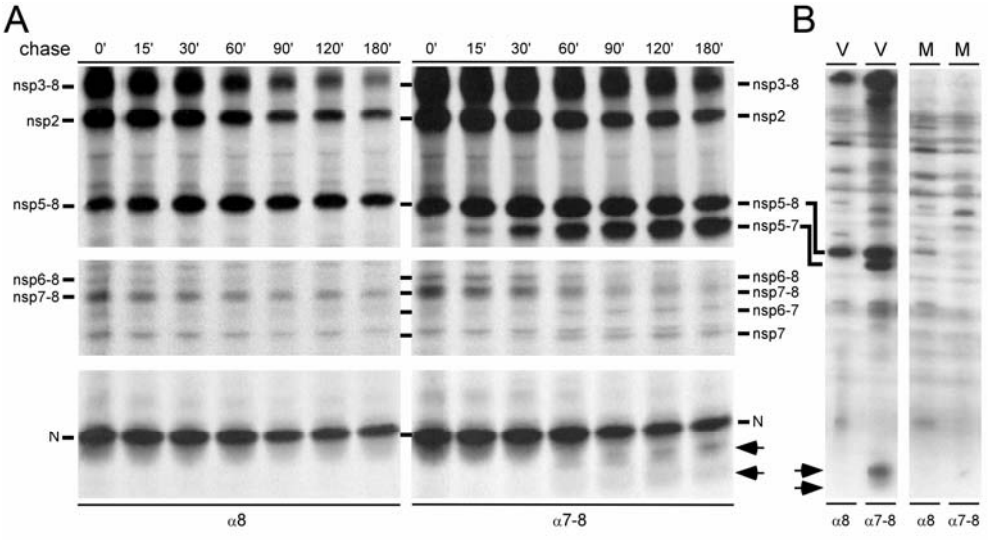

Figure 7.3. Pulse-chase and Western blot analysis of EAV infected cells. (**A**) Pulse-chase experiment analyzing expressed proteins of EAV-infected cells immunoprecipitated with a nsp8 antiserum (left panel) and a nsp7-8 antiserum (right panel). (**B**) Western blot analysis of EAV infected BHK-cells (V) and mock infected cells (M) with either the anti-nsp8 serum or the anti-nsp7-8 serum 8 h post infection. Possible minor processing products in the 13-16 kDa size range (indicated by arrows) were detected only using the anti-nsp7-8 serum.

Analysis of internal processing of the nsp7 region in a transient expression system

To assess the possibility of an internal cleavage in EAV nsp7 in more detail, we re-evaluated pp1a processing upon transient expression of the wild-type protein and the five P1 Glu→Pro mutants mentioned above (E1064P, E1268P, E1430P, E1452P and E1677P; Table 1) (Snijder *et al.*, 1996; Wassenaar *et al.*, 1997). In particular, we looked for processing products in the 13-16 kDa size range that were recognized by the anti-nsp7-8 serum (Fig. 7.4A). For convenience, from this point forward, we will refer to the cleavage products representing the N- and C-terminal parts of nsp7 as nsp7α and nsp7β, respectively, and to the postulated novel cleavage site as the nsp7α/7β site. Unfortunately, nsp7ß (predicted size ~12 kDa) was not detected in our analyses, which may have been due to its low methionine content (Fig. 7.4B), high turnover or further processing of this product, or to comigration with background bands present in the gel (Fig. 7.4A).

As shown in Fig. 7.2, mutant E1677P yielded products of ~14 and ~15 kDa (Fig. 7.4A, lane 7). The ~15-kDa product was not produced by any of the other constructs, which was in line with the hypothesis that it was the C-terminal nsp7 cleavage product (nsp7ß) that could only be visualized when fused to nsp8 (nsp7ß-8; Fig. 7.4B). Also, the incorporation of [^{35}S]-label into nsp7α and nsp7β-8, as determined by phosphorimager analysis, nicely reflected the methionine content of the two products (3:2; Fig. 7.4B). The same analysis also revealed an approximately 60% increase of the nsp7α level compared to that of the wild-type control, suggesting that the block at the nsp7/8 cleavage site promoted cleavage of the nsp7α/7β junction. For the nsp6/7 cleavage site mutant E1452P (Fig. 7.4A, lane 6) the ~14-kDa product shifted to a size of about 16 kDa, suggesting that it indeed

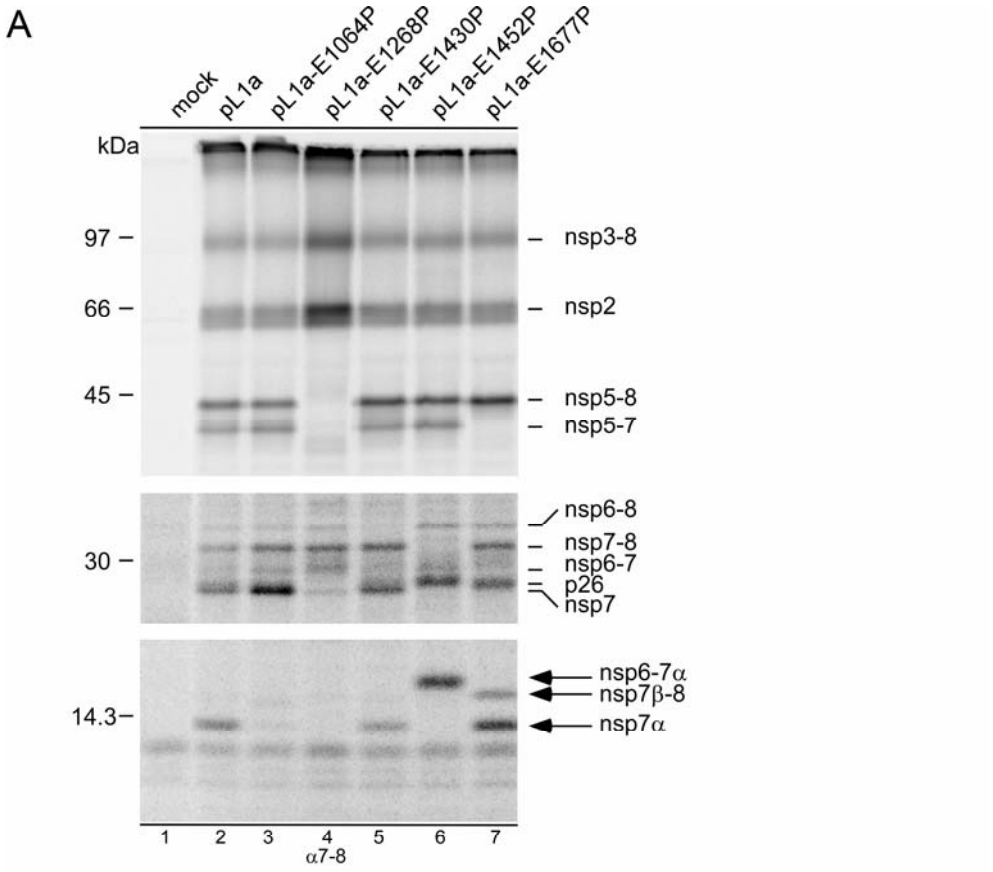

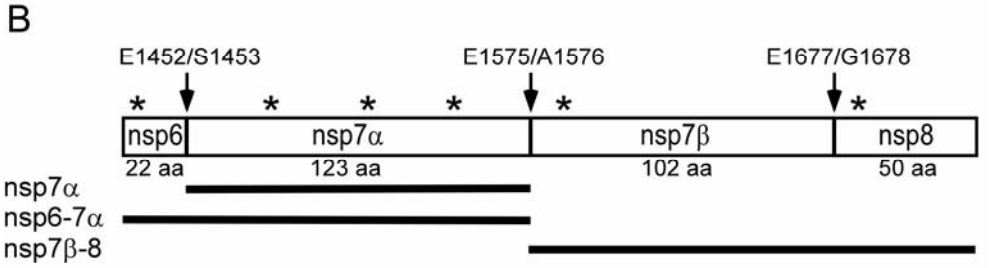

C

```
NC_002532_EAV-Buc   :AKVVGGSRCTICDVV----------KESANDTPVKPMPSRRRRKGLPKGAQLEWDRHQEEKRNAGDDDFAVSNDYVGRVP  :1558-1627
NC_003092_SHFV      :SHPVGGTICTLCVVQ----------AKCSGG---LVTQVNGKFSPAKYLAVAGKVLADH-PDYKLENDGRFPRTREDRVCD  :1956-2022
NC_002534_LDV       :ARTVAGTQFSVGTIC----------GDLSNACEDP----------------------SGLV-KTSKKQAR---RGQCR  :2028-2051
AF325691_PRRSV-NVS  :ARVVAGSKMTVARVVDPTPTPPPEPVPIPLPPKILSNG----------------------PNAW-GDEDLRNK---KKRCR  :2313-2367
AY366525_PRRSV-Eur  :ARSIGGSKFSVCTVVSNTPVDALTGIPLQTPTPLFSNG----------------------PRHR-SEEDDLKV---EGMCK  :2179-2233
```

Figure 7.4. (**A**) **Immunoprecipitation analysis of transient expression of wild-type EAV pp1a and five nsp4 cleavage site mutants after a 5 h interval labelling using an anti-nsp7-8 serum.** The position of the molecular mass markers used during SDS-PAGE and the various processing products are indicated. Note that different exposure times were used for different panels. (**B**) **Tentative processing scheme of the EAV nsp6-8 region.** Based on the findings in Fig. 7.4A, an internal cleavage site near the centre of nsp7 was postulated. The number of methionines and their relative positions in the fragments are indicated with a "*". (**C**) **Multiple alignment of the central domain of nsp7 of selected arteriviruses.** A potential, conserved nsp4 cleavage site was identified in EAV pp1a at position Glu-1575/Ala-1576. Background color: black, invariant residues; dark, grey and light grey, residues conserved in 100%, 75% or 50% of the sequences, respectively. Conservation groups: I,V,L,M; F,Y; K,R; D, N; E,Q; S, T. NC_002532_EAV-Buc, equine arteritis virus strain Bucyrus (den Boon *et al.*, 1991). NC_003092_SHFV, simian hemorrhagic fever virus strain LVR 42-0/M6941 (Zeng *et al.*, 1995). NC_002534_LDV, lactate dehydrogenase-elevating virus strain neurovirulent type C (Godeny *et al.*, 1993). AF325691_PRRSV-NVS, porcine reproductive and respiratory syndrome virus isolate NVSL 97-7985 IA 1-4-2 (Shen *et al.*, 2000), strain AY366525_PRRSV-Eur, porcine reproductive and respiratory syndrome virus strain EuroPRRSV (Ropp *et al.*, 2004).

represented an N-terminal fragment of nsp7 that had now become N-terminally extended with nsp6 (22 amino acids; Fig. 7.4B) to give nsp6-7α. In view of the increased amount of nsp7α in this lane, also this mutation appeared to promote cleavage of the nsp7α/7β site.

The E1452P and E1677P mutants also produced a novel band of approximately 26 kDa (p26) that we cannot readily explain (Fig. 7.4B). The same product was observed upon expression of several other pp1a mutants with altered processing of the nsp3-8 region (unpublished data). The slight migration difference between these two minor bands suggests that the product may in fact contain one of the mutations and thus be derived from the nsp6-8 region itself, e.g. by cleavage at an alternative site when one of the default cleavage sites is blocked. Alternatively, the bands could represent products from another part of the polyprotein or could even be host proteins whose synthesis or co-immunoprecipitation is somehow promoted by the disturbed processing of the nsp6/7 and nsp7/8 junctions.

Interestingly, in the case of mutant E1064P, which does not process the nsp3/4 site, nsp7 accumulated and only a small amount of nsp7α was observed. In the light of this observation, it is tempting to speculate that nsp7α derives from a processing step that occurs predominantly in *trans* and is facilitated by the release of nsp4 from nsp3. This hypothesis is in line with the fact that also the cleavage of the nsp3-4 intermediate, which is probably membrane-associated due to the hydrophobic properties of nsp3, is a relatively late event in pp1a maturation (Snijder *et al.*, 1994). Likewise in mutant E1268P, in which the nsp4/5 cleavage was blocked and the nsp4 enzyme remained attached to another putative trans-membrane protein (nsp5), nsp7α was not observed and also very little nsp7 was accumulated. Similar processing differences in alternative forms of a viral protease have been described previously for the poliovirus 3C enzyme (3C versus 3CD) (Jore *et al.*, 1988; Ypma-Wong *et al.*, 1988) and were, like our observations, implicated in the fine-tuning of polyprotein processing that is required to regulate the viral life cycle. Formally, we cannot exclude that the nsp3/4 and nsp4/5 cleavage site mutations affected the substrate(s) rather than the enzyme necessary to produce nsp7α. However, we consider this less likely since the production of nsp7α was not significantly affected by a block at the nsp5/6 cleavage site (mutant E1430P; Fig. 7.4A, lane 5), which is closer to nsp7α than the two other cleavage sites probed.

Identification of a putative internal cleavage site in nsp7

The data presented thus far suggested an internal nsp4-driven cleavage in the central region of nsp7. Using the apparent molecular weights of the processing products in Fig. 7.4A, we arrived at a processing map for the nsp6-8 precursor that was consistent with all data obtained so far (Fig. 7.4B). Based on the observed product sizes, the novel internal cleavage site in nsp7 was estimated to be located about 125 amino acids downstream of the N-terminal Ser-1453 of the protein. Based on the preference of arterivirus main proteases to cleave between a Glu at P1 and a small amino acid (Gly/Ala/Ser) at P1' (Snijder *et al.*, 1996; Ziebuhr *et al.*, 2000), a potential cleavage site was identified at position E1575/A1576 in EAV pp1a (Fig. 7.4C). Cleavage of the E1575/A1576 junction in fully processed nsp7 would yield an N-terminal product (nsp7α) with a calculated molecular mass of 13.5 kDa, an excellent match with the ~14-kDa product recognized by the anti-nsp7-8 serum in Fig. 7.2 to 4.

A revised alignment of a representative set of arterivirus nsp7 sequences revealed that this site is located in an extremely divergent region of the replicase polyprotein. Nevertheless, each arterivirus examined was found to have a potential counterpart for this site (Fig. 7.4C and data not shown). The P1 Glu-1575 matched Glu residues in all other arterivirus sequences, whereas the P1' Ala-1576 could be aligned with Gly or Asn in the other sequences. Whereas Gly is found at the P1' position in many arterivirus nsp4 cleavage sites (Ziebuhr *et al.*, 2000), the results presented in Fig. 7.2 and Table 1 indicated that Asn at P1' can also be tolerated. Thus, the Glu-1575/Ala-1576 dipeptide was concluded to comply with the P1-P1' preferences of the arterivirus main protease. The poor sequence conservation around this candidate cleavage site explains why it was missed in previous comparative sequence analyses.

To test the above prediction, mutagenesis of the putative nsp7α/7β site was conducted, anticipating that this would allow us to block of nsp7α production. To this end, a P1 Glu-1575→Ala substitution was introduced in pp1a expression vector pL1a. However, since position 1574 is also occupied by a Glu residue, this change created an alternative potential cleavage site (Glu-1574/Ala-1575) in the mutant (besides the P1/P1' signature, no other determinants have been identified in arterivirus nsp4 substrates). In order to preclude processing of this alternative substrate, a second Glu→Ala mutation was introduced in an additional construct (double mutant E1574A/E1575A), changing the original Glu-Glu-Ala sequence into Ala-Ala-Ala. The two mutant proteins were transiently expressed as described in Materials and methods and processing of the nsp7α/7β site was analyzed by immunoprecipitation with the anti-nsp7-8 serum, which had been shown to bring down nsp7α (Fig. 7.2B).

Indeed, production of nsp7α was affected in both mutants, but was only completely inhibited in case of the double mutant (Fig. 7.2B, lane 9). The single Glu-1575→Ala mutation allowed some residual cleavage, possibly - as explained above - due to the cleavage of the artificial Glu-1574/Ala-1575 junction created by the mutation. This would also explain the observation that nsp7α of this mutant, now being one amino acid shorter, migrated slightly faster (Fig. 7.2B, lane 8). Taken together, our theoretical analysis and experimental data strongly supported the identification of Glu-1575/Ala-1576 as the probable nsp7α/7β cleavage site in EAV.

Reverse genetics data support the importance of the internal processing of nsp7

As described in the first paragraph for the other P1 mutations (at the nsp3/4 to nsp7/8 sites), the effect of mutations at the putative nsp7α/7β cleavage site (E1575A and E1574A/E1575A) was tested in the EAV reverse genetics system (Table 1). In repeated experiments, both mutants did not express nsp3 or nucleocapsid (N) protein at 13 h post transfection and did not produce infectious progeny. However, in one experiment, apparent reversion (or pseudoreversion) was observed for mutant E1575A in a 24 h post transfection IFA, suggesting that this mutant possesses some residual RNA synthesis activity. Thus, the reverse genetics analysis revealed the general importance of Glu-1575 for EAV viability. On the basis of the data presented in the previous paragraphs, we propose that this is due to its role as P1 residue of the novel nsp7α/7β site, which implies that also this relatively late and minor processing step is critical for virus reproduction.

Polyprotein 1a processing is critical for EAV RNA synthesis

The proteolytic processing map of the EAV replicase polyproteins was previously thought to be complete. However, several lines of evidence now point towards the occurrence of an additional nsp4-mediated cleavage in nsp7. Although the C-terminal product of this cleavage (nsp7ß) was only detected indirectly (when extended with nsp8 in the case of mutant E1677P; Fig. 7.2A), nsp7α was observed both in infected cells and in expression systems. The position of the novel products in the replicase processing scheme (Fig. 7.4B) was supported by their recognition by specific antisera, the size changes upon mutagenesis of flanking cleavage sites (Fig. 7.4A), and the identification of a conserved potential nsp7α/7ß cleavage site (Fig. 7.4C), whose mutagenesis indeed prevented the production of nsp7α (Fig. 7.2B). As in the case of the other nsp4 cleavage sites tested in this study (Table 1), mutagenesis of the putative P1 residue (Glu-1575) of the novel site was found to be critical for EAV RNA synthesis.

Mutations in specific EAV replicase subunits were previously found to selectively affect subgenomic RNA synthesis (van Dinten *et al.*, 1997; Tijms *et al.*, 2001). However, our *in vivo* assessment of the importance of nsp4-mediated processing of the nsp3-8 region showed that mutants in which cleavage of one of the six sites was blocked are all equally impaired in terms of both genome replication and subgenomic mRNA synthesis, suggesting that both the major and the minor processing pathways are essential for viral RNA synthesis. Even more than before, it has become clear that the EAV nsp3-8 region is processed extensively and in a highly regulated fashion, to produce a variety of overlapping processing intermediates and relatively small end products.

A wide variety of nsp7-containing cleavage products is produced by arteriviruses

The function of nsp7 in the arterivirus life cycle is currently unknown and so far no homolog of the protein has been identified in other virus systems. The internal processing of nsp7 suggests that nsp7 consists of two smaller subdomains. Nsp7α and nsp7ß may cooperate to fulfil a joint nsp7 function or may each have a separate function. The number of currently identified processing intermediates that contain EAV nsp7 is remarkable. In certain products (nsp6-8, nsp6-7 and nsp7-8) nsp7 is N- and/or C-terminally extended by

the flanking small proteins nsp6 (22 aa) and nsp8 (50 aa), which may thus modulate its function. In the nsp3-8, nsp5-8, and nsp5-7 intermediates, nsp7 is connected to one or multiple hydrophobic domains (nsp3 and/or nsp5 (Snijder *et al.*, 1994)). Finally, due to its position just upstream of the ribosomal frameshift site, nsp7 is part of large processing intermediates that extend into the ORF1b-encoded part of the replicase, in particular including the nsp9 RNA-dependent RNA polymerase (van Dinten *et al.*, 1996; van Dinten *et al.*, 1999). Possibly, these long-lived nsp7-containing intermediates play different roles in EAV RNA synthesis.

In the distantly related corona- and toroviruses, the corresponding region of pp1a, which displays no recognizable sequence similarity to that of arteriviruses, is also processed into several small proteins by the main protease (Ziebuhr *et al.*, 2000; Gorbalenya *et al.*, 2006; Smits *et al.*, 2006). In coronaviruses, this region encompasses nsp7 to nsp10 and it was demonstrated that these proteins colocalize in replication complexes with the viral helicase, nucleocapsid protein and 3C-like protease (Bost *et al.*, 2000; Snijder *et al.*, 2006). Recently, genetic studies have implicated nsp10 in viral RNA synthesis (Sawicki *et al.*, 2005) and crystallographic studies showed that nsp9 is an RNA-binding protein (Egloff *et al.*, 2004; Sutton *et al.*, 2004). Furthermore, nsp7 and nsp8 have been shown to form a hexadecameric supercomplex that is capable of encircling RNA and may operate as a cofactor in viral RNA synthesis (Zhai *et al.*, 2005). It will be very interesting to see whether this part of the arterivirus replicase polyprotein, despite the lack of a clear phylogenetic relationship, has evolved to be the functional equivalent of the corresponding region of the coronavirus replicase polyprotein.

Acknowledgments

The authors would like to thank Dmitry Samborskiy for making the Viralis platform operational, Marieke Tijms for technical assistance, and Fred Wassenaar and Willy Spaan for helpful discussions and support. D.v.A was supported by a grant from the Leiden University Stimuleringsfonds.

Reference List

1. **Anand, K., Palm, G. J., Mesters, J. R., Siddell, S. G., Ziebuhr, J. & Hilgenfeld, R. (2002).** Structure of coronavirus main proteinase reveals combination of a chymotrypsin fold with an extra alpha-helical domain. *EMBO J* **21**, 3213-3224
2. **Barrette-Ng, I. H., Ng, K. K. S., Mark, B. L., van Aken, D., Cherney, M. M., Garen, C., Kolodenko, Y., Gorbalenya, A. E., Snijder, E. J. & James, M. N. G. (2002).** Structure of arterivirus nsp4 - The smallest chymotrypsin-like proteinase with an alpha/beta C-terminal extension and alternate conformations of the oxyanion hole. *J Biol Chem* **277**, 39960-39966
3. **Bartenschlager, R., Ahlborn-Laake, L., Mous, J. & Jacobsen, H. (1994).** Kinetic and structural analyses of hepatitis C virus polyprotein processing. *J Virol* **68**, 5045-5055
4. **Bost, A. G., Carnahan, R. H., Lu, X. T. & Denison, M. R. (2000).** Four proteins processed from the replicase gene polyprotein of mouse hepatitis virus colocalize in the cell periphery and adjacent to sites of virion assembly. *J Virol* **74**, 3379-3387
5. **de Vries, A. A. F., Chirnside, E. D., Horzinek, M. C. & Rottier, P. J. (1992).** Structural proteins of equine arteritis virus. *J Virol* **66**, 6294-6303
6. **den Boon, J. A., Snijder, E. J., Chirnside, E. D., de Vries, A. A. F., Horzinek, M. C. & Spaan, W. J. M. (1991).** Equine arteritis virus is not a togavirus but belongs to the coronaviruslike superfamily. *J Virol* **65**, 2910-2920
7. **Denison, M. R., Yount, B., Brockway, S. M., Graham, R. L., Sims, A. C., Lu, X. & Baric, R. S. (2004).** Cleavage between replicase proteins p28 and p65 of mouse hepatitis virus is not required for virus replication. *J Virol* **78**, 5957-5965
8. **Ding, M. X. & Schlesinger, M. J. (1989).** Evidence that Sindbis virus NSP2 is an autoprotease which processes the virus nonstructural polyprotein. *Virology* **171**, 280-284
9. **Doll, E. R., Bryans, J. T., McCollum, W. H. & Wallace, M. E. (1957).** Isolation of a filterable agent causing arteritis of horses and abortion by mares; its differentiation from the equine abortion (influenza) virus. *Cornell Vet* **47**, 3-41
10. **Edgar, R. C. (2004).** MUSCLE: multiple sequence alignment with high accuracy and high throughput. *Nucleic Acids Res* **32**, 1792-1797
11. **Egloff, M. P., Ferron, F., Campanacci, V., Longhi, S., Rancurel, C., Dutartre, H., Snijder, E. J., Gorbalenya, A. E., Cambillau, C. & Canard, B. (2004).** The severe acute respiratory syndrome-coronavirus replicative protein nsp9 is a single-stranded RNA-binding subunit unique in the RNA virus world. *Proc Natl Acad Sci U S A* **101**, 3792-3796
12. **Fuerst, T. R., Niles, E. G., Studier, F. W. & Moss, B. (1986).** Eukaryotic transient-expression system based on recombinant vaccinia virus that synthesizes bacteriophage T7 RNA polymerase. *Proc Natl Acad Sci U S A* **83**, 8122-8126
13. **Godeny, E. K., Chen, L., Kumar, S. N., Methven, S. L., Koonin, E. V. & Brinton, M. A. (1993).** Complete genomic sequence and phylogenetic analysis of the lactate dehydrogenase-elevating virus (LDV). *Virology* **194**, 585-596

14. **Gorbalenya, A. E., Enjuanes, L., Ziebuhr, J. & Snijder, E. J. (2006).** Nidovirales: evolving the largest RNA virus genome. *Virus Res* **117**, 17-37
15. **Gorbalenya, A. E. & Snijder, E. J. (1996).** Viral cysteine proteases. *Persp Drug Discov Design* **6**, 64-86
16. **Hardy, M. E., Crone, T. J., Brower, J. E. & Ettayebi, K. (2002).** Substrate specificity of the Norwalk virus 3C-like proteinase. *Virus Res* **89**, 29-39
17. **Jore, J., De Geus, B., Jackson, R. J., Pouwels, P. H. & Enger-Valk, B. E. (1988).** Poliovirus protein 3CD is the active protease for processing of the precursor protein P1 in vitro. *J Gen Virol* **69**, 1627-1636
18. **Kim, J. C., Spence, R. A., Currier, P. F., Lu, X. & Denison, M. R. (1995).** Coronavirus protein processing and RNA synthesis is inhibited by the cysteine proteinase inhibitor E64d. *Virology* **208**, 1-8
19. **Laemmli, U. K. (1970).** Cleavage of structural proteins during the assembly of the head of bacteriophage T4. *Nature* **227**, 680-685
20. **Landt, O., Grunert, H.-P. & Hahn, U. (1990).** A general method for rapid site-directed mutagenesis using the polymerase chain reaction. *Gene* **96:** 125-128
21. **Ropp, S. L., Wees, C. E., Fang, Y., Nelson, E. A., Rossow, K. D., Bien, M., Arndt, B., Preszler, S., Steen, P., Christopher-Hennings, J. & other authors. (2004).** Characterization of emerging European-like porcine reproductive and respiratory syndrome virus isolates in the United States. *J Virol* **78**, 3684-3703
22. **Rose, J. R., Babe, L. M. & Craik, C. S. (1995).** Defining the level of human immunodeficiency virus type 1 (HIV-1) protease activity required for HIV-1 particle maturation and infectivity. *J Virol* **69**, 2751-2758
23. **Ryan, M. D. & Flint, M. (1997).** Virus-encoded proteinases of the picornavirus super-group. *J Gen Virol* **78 (Pt 4)**, 699-723
24. **Sambrook, J., E. F. Fritsch & T. Maniatis (1989).** Molecular cloning: a laboratory manual, 2nd edn. Cold Spring Harbor, N.Y.: Cold Spring Harbor Laboratory Press.
25. **Sawicki, S. G., Sawicki, D. L., Younker, D., Meyer, Y., Thiel, V., Stokes, H. & Siddell, S. G. (2005).** Functional and genetic analysis of coronavirus replicase-transcriptase proteins. *PLoS Pathog* **1**, e39
26. **Schechter, I. & Berger, A. (1967).** On the size of the active site in proteases. I. Papain. *Biochem Biophys Res Commun* **27**, 157-162
27. **Shen, S., Kwang, J., Liu, W. & Liu, D. X. (2000).** Determination of the complete nucleotide sequence of a vaccine strain of porcine reproductive and respiratory syndrome virus and identification of the Nsp2 gene with a unique insertion. *Arch Virol* **145**, 871-883
28. **Siddell, S. G., J. Ziebuhr & E. J. Snijder (2005).** In *Topley and Wilson's microbiology and microbial infections*, Virology volume, 10th edn, pp. 823-856. Edited by B. W. Mahy & V. ter Meulen. London: Hodder Arnold.
29. **Smits, S. L., Snijder, E. J. & de Groot, R. J. (2006).** Characterization of a torovirus main proteinase. *J Virol* **80**, 4157-4167
30. **Snijder, E. J., M. A. Brinton, K. S. Faaberg, E. K. Godeny, A. E. Gorbalenya, N. J. MacLachlan, W. L. Mengeling & P. G. W. Plagemann (2005).** In *Virus Taxonomy, 8th Report of the ICTV*, pp. 965-974. Edited by C. M. Fauqet, M. A. Mayo, J. Maniloff, U. Desselberger & L. A. Ball. London: Elsevier/Academic Press.

31. **Snijder, E. J., Dobbe, J. C. & Spaan, W. J. M. (2003).** Heterodimerization of the two major envelope proteins is essential for arterivirus infectivity. *J Virol* **77**, 97-104
32. **Snijder, E. J. & Meulenberg, J. J. M. (1998).** The molecular biology of arteriviruses. *J Gen Virol* **79**, 961-979
33. **Snijder, E. J. & J. J. M. Meulenberg (2001).** In *Fields Virology*, 4th edn, pp. 1205-1220. Edited by D. M. Knipe & P. M. Howley. Philadelphia: Lippincott, Williams & Wilkins.
34. **Snijder, E. J., van der Meer, Y., Zevenhoven-Dobbe, J., Onderwater, J. J. M., van der Meulen, J., Koerten, H. K. & Mommaas, A. M. (2006).** Ultrastructure and origin of membrane vesicles associated with the severe acute respiratory syndrome coronavirus replication complex. *J Virol* **80**, 5927-5940
35. **Snijder, E. J., Wassenaar, A. L. M., van Dinten, L. C., Spaan, W. J. M. & Gorbalenya, A. E. (1996).** The arterivirus nsp4 protease is the prototype of a novel group of chymotrypsin-like enzymes, the 3C-like serine proteases. *J Biol Chem* **271**, 4864-4871
36. **Snijder, E. J., Wassenaar, A. L. M. & Spaan, W. J. M. (1994).** Proteolytic processing of the replicase ORF1a protein of equine arteritis virus. *J Virol* **68**, 5755-5764
37. **Spaan, W. J. M., D. Cavanagh, R. J. de Groot, L. Enjuanes, A. E. Gorbalenya, E. J. Snijder & P. J. Walker (2005).** In *Virus Taxonomy, 8th Report of the ICTV*, pp. 937-945. Edited by C. M. Fauqet, M. A. Mayo, J. Maniloff, U. Desselberger & L. A. Ball. London: Elsevier/Academic Press.
38. **Sutton, G., Fry, E., Carter, L., Sainsbury, S., Walter, T., Nettleship, J., Berrow, N., Owens, R., Gilbert, R., Davidson, A. & other authors. (2004).** The nsp9 replicase protein of SARS-coronavirus, structure and functional insights. *Structure* **12**, 341-353
39. **Tijms, M. A., van Dinten, L. C., Gorbalenya, A. E. & Snijder, E. J. (2001).** A zinc finger-containing papain-like protease couples subgenomic mRNA synthesis to genome translation in a positive-stranded RNA virus. *Proc Natl Acad Sci U S A* **98**, 1889-1894
40. **van Aken, D., Benckhuijsen, W. E., Drijfhout, J. W., Wassenaar, A. L., Gorbalenya, A. E. & Snijder, E. J. (2006a).** Expression, purification, and in vitro activity of an arterivirus main proteinase. *Virus Res*
41. **van Aken, D., Snijder, E. J. & Gorbalenya, A. E. (2006b).** Mutagenesis analysis of the nsp4 main proteinase reveals determinants of arterivirus replicase polyprotein autoprocessing. *J Virol* **80**, 3428-3437
42. **van der Meer, Y., van Tol, H., Locker, J. K. & Snijder, E. J. (1998).** ORF1a-encoded replicase subunits are involved in the membrane association of the arterivirus replication complex. *J Virol* **72**, 6689-6698
43. **van Dinten, L. C., den Boon, J. A., Wassenaar, A. L. M., Spaan, W. J. M. & Snijder, E. J. (1997).** An infectious arterivirus cDNA clone: identification of a replicase point mutation that abolishes discontinuous mRNA transcription. *Proc Natl Acad Sci U S A* **94**, 991-996
44. **van Dinten, L. C., Rensen, S., Gorbalenya, A. E. & Snijder, E. J. (1999).** Proteolytic processing of the open reading frame 1b-encoded part of arterivirus replicase is mediated by nsp4 serine protease and Is essential for virus replication. *J Virol* **73**, 2027-2037

45. **van Dinten, L. C., Wassenaar, A. L. M., Gorbalenya, A. E., Spaan, W. J. M. & Snijder, E. J. (1996).** Processing of the equine arteritis virus replicase ORF1b protein: identification of cleavage products containing the putative viral polymerase and helicase domains. *J Virol* **70**, 6625-6633
46. **Wassenaar, A. L. M., Spaan, W. J. M., Gorbalenya, A. E. & Snijder, E. J. (1997).** Alternative proteolytic processing of the arterivirus replicase ORF1a polyprotein: evidence that NSP2 acts as a cofactor for the NSP4 serine protease. *J Virol* **71**, 9313-9322
47. **Yang, H., Xie, W., Xue, X., Yang, K., Ma, J., Liang, W., Zhao, Q., Zhou, Z., Pei, D., Ziebuhr, J. & other authors**. **(2005).** Design of wide-spectrum inhibitors targeting coronavirus main proteases. *PLoS Biol* **3**, e324
48. **Yang, H., Yang, M., Ding, Y., Liu, Y., Lou, Z., Zhou, Z., Sun, L., Mo, L., Ye, S., Pang, H. & other authors**. **(2003).** The crystal structures of severe acute respiratory syndrome virus main protease and its complex with an inhibitor. *Proc Natl Acad Sci U S A* **100**, 13190-13195
49. **Ypma-Wong, M. F., Dewalt, P. G., Johnson, V. H., Lamb, J. G. & Semler, B. L. (1988).** Protein 3Cd Is the Major Poliovirus Proteinase Responsible for Cleavage of the P1 Capsid Precursor. *Virology* **166**, 265-270
50. **Zeng, L., Godeny, E. K., Methven, S. L. & Brinton, M. A. (1995).** Analysis of simian hemorrhagic fever virus (SHFV) subgenomic RNAs, junction sequences, and 5' leader. *Virology* **207**, 543-548
51. **Zhai, Y., Sun, F., Li, X., Pang, H., Xu, X., Bartlam, M. & Rao, Z. (2005).** Insights into SARS-CoV transcription and replication from the structure of the nsp7-nsp8 hexadecamer. *Nat Struct Mol Biol* **12**, 980-986
52. **Ziebuhr, J., Bayer, S., Cowley, J. A. & Gorbalenya, A. E. (2003).** The 3C-like proteinase of an invertebrate nidovirus links coronavirus and potyvirus homologs. *J Virol* **77**, 1415-1426
53. **Ziebuhr, J., Snijder, E. J. & Gorbalenya, A. E. (2000).** Virus-encoded proteinases and proteolytic processing in the *Nidovirales*. *J Gen Virol* **81**, 853-879